Published in final edited form as:
Brain Res. 2008 November 13; 1240: 185–195. doi:10.1016/j.brainres.2008.08.089.

Measures of striatal insulin resistance in a 6-hydroxydopamine model of Parkinson's Disease

Jill K. Morris[1], **Hongyu Zhang**[1], **Anisha A. Gupte**[1], **Greg L. Bomhoff**[1], **John A. Stanford**[1,2,3], and **Paige C. Geiger**[1,2,3,*]

1*Department of Molecular & Integrative Physiology, University of Kansas Medical Center, Kansas City, KS 66160*

2*Landon Center on Aging, University of Kansas Medical Center, Kansas City, KS 66160*

3*Kansas Intellectual & Developmental Disabilities Research Center, University of Kansas Medical Center, Kansas City, KS 66160*

Abstract

Clinical evidence has shown a correlation between Parkinson's Disease (PD) and Type 2 Diabetes (T2D), as abnormal glucose tolerance has been reported in >50% of PD patients. The development of insulin resistance and the degeneration of nigrostriatal dopamine (DA) neurons are both mediated by oxidative mechanisms, and oxidative stress is likely a mechanistic link between these pathologies. Although glucose uptake in neuronal tissues is primarily non-insulin dependent, proteins involved in insulin signaling, such as insulin receptor substrate 2 (IRS2) and glucose transporter 4 (GLUT4), are present in the basal ganglia. The purpose of this study was to determine whether nigrostriatal DA depletion affects measures of insulin resistance in the striatum. Six weeks after 6-hydroxydopamine (6-OHDA) infusion into the medial forebrain bundle, rats were classified as having either partial (20–65%) or severe (90–99%) striatal DA depletion. Increased IRS-2 serine phosphorylation, a marker of insulin resistance, was observed in the DA depleted striatum. Additionally, severe depletion resulted in decreased total IRS-2, indicating possible degradation of the protein. Decreased phosphorylation of AKT and expression of the kinase glycogen synthase kinase-3 alpha (GSK3-α) was also measured in the striatum of severely DA depleted animals. Finally, expression of heat shock protein 25 (hsp25), which is protective against oxidative damage and can decrease stress kinase activity, was decreased in the striatum of lesioned rats. Together, these results support the hypothesis that nigrostriatal DA depletion impairs insulin signaling in the basal ganglia.

Keywords

Parkinson's disease; animal models; insulin signaling; diabetes; IRS2; basal ganglia; striatum; glucose

*Correspondence to: Paige C. Geiger, Ph.D., Department of Physiology, Mailstop 3051, University of Kansas Medical Center, 3901 Rainbow Blvd., Kansas City, KS 66160, phone: 913-588-7408, email: pgeiger@kumc.edu.

I. Introduction

Parkinson's disease (PD) is characterized by degeneration of dopaminergic neurons projecting from the substantia nigra pars compacta (SNpc) to the striatum. This degeneration results in decreased striatal dopamine (DA) content, aberrant neurotransmission throughout the basal ganglia, and motor dysfunction. PD patients also exhibit autonomic and endocrine deficits, such as glucose intolerance and diabetes (Barbeau and Pourcher, 1982; Boyd et al., 1971; Lipman et al., 1974). Insulin resistance, often characterized by impaired insulin signal transduction, diminished glucose uptake, and dysregulated energy metabolism, is frequently preceded by glucose intolerance and can lead to the development of Type 2 Diabetes (T2D).

Clinical studies have revealed a high incidence of glucose intolerance (>50%) in PD (Sandyk, 1993). It has been shown that patients with PD exhibit increased autoimmune reactivity to insulin (Wilhelm et al., 2007), and that PD patients with diabetes have increased PD disease severity (Papapetropoulos et al., 2004). Co-morbidity of PD and T2D is also correlated with a significant increase in the cost of care of affected individuals (Pressley et al., 2003). Hyperglycemia has been suggested to decrease the effectiveness of levodopa (L-DOPA) therapy and increase motor dyskinesias experienced by PD patients (Sandyk, 1993). Further, L-DOPA therapy may exacerbate hyperinsulinemia and hyperglycemia in PD patients (Boyd et al., 1971; Sirtori et al., 1972), possibly by diminishing peripheral glucose disposal in skeletal muscle (Smith et al., 2004). An early marker for the development of peripheral glucose intolerance may be insulin resistance in neural tissues. Hypothalamic parasympathetic nerves affect insulin release by beta cells, while sympathetic nerves act directly on the liver to affect hepatic glucose metabolism (reviewed in (Uyama et al., 2004)). Thus, it is important to understand the mechanistic link between nigrostriatal DA depletion and CNS insulin signaling.

Studies indicate a role for insulin signaling in the basal ganglia. Insulin receptors co-localize with neurons containing tyrosine hydroxylase in the SNpc (Figlewicz et al., 2003; Moroo et al., 1994), and mRNA for insulin receptor is present in human SN (Takahashi et al., 1996). Insulin receptor substrate 2 (IRS2) is also present in the CNS and functions to couple insulin receptor activation to signaling via the IRS-PI3K pathway (Porte et al., 2005). Finally, localization of the insulin-dependent glucose transporter GLUT4 to the brain, including basal ganglia nuclei (El Messari et al., 1998), suggests an important role for insulin signaling in neuronal function. Despite these findings and their clinical implications, preclinical studies examining relationships between nigrostriatal DA depletion and insulin resistance in animal models are lacking.

The purpose of the current study was to test the hypothesis that nigrostriatal dopamine depletion following unilateral 6-hydroxydopamine (6-OHDA) infusion would impair insulin signaling in the basal ganglia. The unilateral 6-OHDA-treated rat is perhaps the most widely studied preclinical model of PD, and the effects of this model on nigrostriatal DA are well documented (Schober, 2004; Yuan et al., 2005). Because insulin resistance has been tied to a post-insulin receptor defect in insulin signaling (Fink et al., 1983), in the current study we measured the expression and activation of proteins involved in post-receptor insulin signaling, including IRS2, AKT, JNK, GSK3-α/β, and Hsp25. To our knowledge, this study is the first to assess brain insulin signaling in the 6-OHDA preclinical model of PD.

2. Results

2.1. Body weight

The Fisher 344 rats used in this experiment had an average initial body weight of 306.3 ± 8.3g. All three groups gained weight over a period of 6 weeks post-lesion. On average, the percent weight gain was 6.2% for sham lesioned rats, 4.9% for rats with partial DA depletion, and 5.5%

for rats with severe DA depletion. The between-groups differences in weight gain were not significant at 6 weeks post-lesion ($p>0.05$).

2.2. DA depletion

Values for DA and its metabolite dihydroxyphenylacetic acid (DOPAC) in the striatum of animals in each group are given in Table 1. Striatal DA depletion following 6-OHDA ranged from 20–99% (Figure 1). This range is consistent with previous studies using this protocol (Hudson et al., 1993). As previous studies have done (Skitek et al., 1999), we assigned individual rats to groups based on striatal DA depletion levels. Rats exhibiting partial DA depletion (20–65%) were included in the "partial depletion" group (n=6). This group was compared to rats with DA depletions of greater than 90% (n=8), the "severe depletion" group (figure 1). The mean DA depletion for the partial depletion group was 37.6% ± 13.9, while the mean DA depletion for the severe depletion group was 98% ± 2.7%.

2.3. Intraperitoneal glucose tolerance test (IPGTT)

An IPGTT was performed to determine if severe DA depletion affects peripheral glucose tolerance six weeks post-lesion. An IPGTT was not performed on partially lesioned animals. Both serum insulin levels (figure 2A) and blood glucose levels (figure 2B) were measured. A multivariate repeated measures analysis showed no difference in either insulin or glucose levels between groups over the course of the test. However, at one timepoint, (15 minutes), the severely depleted group exhibited an increase in serum insulin that approaches significance ($p=0.06$) that is reflected by a significant decrease in blood glucose ($p=0.04$). No differences were observed between groups at any other timepoint.

2.4. Serine phosphorylation of IRS1 and IRS2

Six weeks post-lesion, rats exhibiting severe DA depletion showed a 69% increase in striatal IRS2 serine phosphorylation ($F=4.238$, $p=0.03$) when compared to both sham lesioned controls (figure 3A). IRS2 serine phosphorylation was also increased with partial DA depletion, although this increase was not significant when compared to the control group. Serine phosphorylation of IRS1 was not significantly different between sham lesion control rats and rats in either lesion group (figure 4A).

2.5. IRS1 and IRS2 protein levels

Serine phosphorylation of IRS1 and IRS2 proteins can result in protein degradation (Kim et al., 2005; Rui et al., 2001). Thus, we evaluated the three experimental groups for total IRS protein content. As expected, the severe DA depletion group that exhibited increased serine phosphorylation also displayed a 47% decrease in total IRS2 protein compared to sham lesioned control rats and a 49% decrease when compared to partially depleted animals ($F=3.603$, $p=0.05$) (figure 3B). IRS2 protein content was not significantly different between the control group and rats exhibiting partial DA depletion. IRS1 total protein levels were not significantly different between any groups (figure 4B).

2.6. Downstream insulin signaling affects

Protein kinase B (AKT) is a major mediator of insulin signaling that functions downstream of IRS proteins (van der Heide et al., 2006). AKT is activated by phosphorylation in response to insulin, and AKT phosphorylation can be used to gauge insulin sensitivity. We observed a 59% decrease in AKT phosphorylation in severely depleted rats compared to sham lesioned controls, (figure 5A) which was statistically significant ($H=6.224$, $p=0.04$). No significant difference in AKT phosphorylation was observed between partially depleted rats and sham lesioned controls.

2.7. Measures of cellular stress

Activation of stress kinases, such as c-Jun N-terminal kinase (JNK) or glycogen synthase kinase 3 (GSK3) in response to a 6-OHDA lesion could contribute to the observed increase in serine phosphorylation in lesioned rats. Lesioned rats exhibiting high levels of DA depletion showed a non-significant increase in JNK phosphorylation six weeks post-lesion (figure 5B). Phosphorylation of GSK3-α and GSK3-β isoforms was also examined. Decreased GSK3 phosphorylation indicates increased kinase activity (Henriksen et al., 2003). A non-significant decrease in GSK3-α and GSK3-β phosphorylation was observed in both partial and severe depletion groups (figure 6A and 6C). However, a significant decrease in GSK3-α protein expression ($H=6.353$, $p=0.04$) was observed in rats exhibiting both partial and severe DA depletion (Figure 6B). GSK3-β expression was not statistically different between either depletion group and control rats (figure 6D). Both depletion groups showed a significant decrease ($H=8.894$, $p=0.02$) in Hsp25 expression. Hsp25 was decreased by 43% in severely depleted rats and 59% in partially depleted animals compared with control rats (figure 7).

3. Discussion

We report here effects on insulin signaling pathways in the basal ganglia following nigrostriatal DA depletion. Signs of impaired insulin signaling in the basal ganglia in rats with severe DA depletion included increased serine phosphorylation of IRS2, decreased IRS2 protein content, and decreased AKT phosphorylation. Decreased GSK3-α and Hsp25 expression were also observed in this group. Animals in the partial depletion group exhibited decreased GSK3-α and Hsp25 expression without a significant effect on IRS2 phosphorylation or expression or AKT phosphorylation. Additionally, a non-significant increase in JNK activation was observed with severe DA depletion, and a non-significant increase in GSK3-α and GSK3-β activation was observed in both depletion groups. At six weeks, no difference in peripheral glucose or insulin levels existed between severely depleted rats and controls over the course of an IPGTT, indicating that a dysfunction in brain insulin signaling may precede changes in peripheral glucose tolerance.

The mechanisms and pathways involved in insulin signal transduction are similar for the periphery and the brain (Reagan, 2005). Insulin signaling requires interactions between IRS proteins and insulin receptor, and these interactions are mediated by the phosphorylation of IRS proteins on tyrosine residues (White, 1998). This process also allows for the binding of effector proteins. Although four IRS isoforms exist, IRS3 and IRS4 are thought to play only minor roles in insulin signaling (Sykiotis and Papavassiliou, 2001) and were not measured in the current study. Conversely, IRS1 and IRS2 are expressed in most tissues and modulate the majority of the insulin signaling in the body (White, 2002). IRS1 is most important in skeletal muscle signaling (Sykiotis and Papavassiliou, 2001), where it has been extensively characterized. Studies have shown IRS2 likely plays a more prominent signaling role in tissues such as liver, pancreas, and brain (Dong et al., 2006; Lin et al., 2004; Taguchi et al., 2007), where its role has been most thoroughly characterized in the hypothalamus (Morton et al., 2007; Pardini et al., 2006; Porte et al., 2005). IRS2 employs an additional interaction with the insulin receptor via its kinase regulatory loop binding domain, allowing discernment between IRS1 and IRS2 signals (Sawka-Verhelle et al., 1997). Serine phosphorylation of IRS1 and IRS2 impairs IRS interaction with the insulin receptor and decreases the ability of these proteins to propagate the insulin signal by undergoing tyrosine phosphorylation (Aguirre et al., 2002; Paz et al., 1997). Our observation of a DA depletion-related increase in IRS2 serine phosphorylation, with little change in serine phosphorylation of IRS1 between either lesion group and sham lesion controls, implicates IRS2 in neural insulin resistance in parkinsonism.

In addition to inhibiting tyrosine phosphorylation, serine phosphorylation of IRS1 and IRS2 can target these proteins for degradation (Kim et al., 2005; Pederson et al., 2001), providing

another mechanism by which insulin signaling can be modified. It has been suggested that IRS1 ubiquitin ligase may associate with a serine kinase which acts on IRS1 (Zhande et al., 2002), and that a partial explanation for decreased insulin signaling in response to serine phosphorylation is proteasome mediated degradation of IRS proteins (Rui et al., 2001; Rui et al., 2002). Our finding of a significant decline in total IRS2 protein in rats with severe DA depletion, but not partial DA depletion, is consistent with increased serine phosphorylation in severely depleted rats. Because IRS2 degradation occurs only with severe and chronic IRS2 serine phosphorylation, it is likely that the non-significant increase in IRS2 serine phosphorylation in the partial depletion group was not sufficient to trigger significant IRS2 degradation. The fact that we observed no difference in total IRS1 protein between lesion and sham lesion groups is consistent with our negative findings regarding expression and activity of IRS1 following DA depletion.

A major mediator of insulin signaling that functions downstream of IRS proteins is AKT (van der Heide et al., 2006). AKT phosphorylation occurs in response to insulin and can be used to gauge insulin sensitivity. AKT activity promotes translocation of the glucose transporter GLUT4 to the plasma membrane (Wang et al., 1999), which allows glucose uptake, and AKT activation is tied to cellular survival (van der Heide et al., 2006). Basal AKT activity also influences DAT expression on the plasma membrane (Garcia et al., 2005). Because of the multifaceted roles of AKT, we analyzed AKT activation in the striatum of 6-OHDA lesioned animals. AKT phosphorylation was significantly decreased in severely depleted rats when compared to sham lesioned controls, indicating a defect in signaling. No significant difference was observed between partially depleted rats and controls.

To investigate a mechanism for increased IRS2 serine phosphorylation, we analyzed two well characterized stress kinases: c-Jun N-terminal kinase (JNK) and glycogen synthase kinase 3 (GSK3). JNK is activated via phosphorylation in response to cellular stress (Bloch-Damti and Bashan, 2005). Specifically, active JNK may contribute to serine phosphorylation of IRS proteins and inhibit insulin signaling (Aguirre et al., 2002; Werner et al., 2004; Zick, 2005). The JNK pathway has also been linked to PD (Peng and Andersen, 2003). JNK contributes to apoptosis of dopaminergic neurons in response to paraquat and rotenone, two neurotoxins used in animal models of PD (Klintworth et al., 2007). Conversely, inhibiting JNK activation facilitates survival of dopaminergic neurons in a 6-OHDA animal model of PD (Rawal et al., 2007). Thus, JNK plays a role in both modulation of insulin signaling and PD pathogenesis. Our data reveal a non-significant increase in active (phosphorylated) JNK in the striatum of severely lesioned rats six weeks post-lesion.

GSK3 is classically known for its role in inhibiting glycogen synthesis by phosphorylating glycogen synthase under basal conditions. Insulin stimulation causes GSK3 phosphorylation, inactivating its kinase activity and allowing glycogen synthesis to occur (Lee and Kim, 2007). However, GSK3 activity has also been suggested to contribute to serine phosphorylation of both IRS1 and IRS2 (Liberman et al., 2008; Sharfi and Eldar-Finkelman, 2008) in rodent models. Two isoforms of GSK3 exist, GSK3-α and GSK3-β. Using Western blot analysis, we measured the phosphorylation levels of both isoforms. A non-significant increase in GSK3-α and GSK3-β activation (decreased phosphorylation) was observed in both depletion groups. GSK3-α expression was significantly decreased in both groups, although no difference in GSK3-β expression was observed. GSK3-β is highly expressed in the central nervous system, where it localizes to neurons (Leroy and Brion, 1999). A previous study reported that 6-OHDA treatment inhibits GSK3-β phosphorylation in a human dopaminergic neuroblastoma cell line and induces GSK3-β dephosphorylation in two additional cell lines (Chen et al., 2004), activating its kinase activity. The role of GSK3-α in the brain has not been as clearly defined but likely exhibits some redundant actions of GSK3-β. GSK inhibition is associated with activation of neuronal survival pathways (Garcia-Segura et al., 2007), and stimulation of

glucose transport (Henriksen et al., 2003), and both isoforms have been implicated in tau phosphorylation in Alzheimer's disease (Baum et al., 1996).

Previous studies have shown Hsp25 (the rodent form of human Hsp27) to be protective against oxidative stress (Escobedo et al., 2004). Specifically, Hsp25 protects against damage to mitochondrial complex I (Downs et al., 1999), which is damaged in PD (Beal, 2003). In addition to its protective role against oxidative damage, Hsp25 has been shown to bind the stress kinase inhibitor of kappa kinase beta (IkKβ), decreasing its activity (Park et al., 2003). Because IkKβ is another stress kinase that is suggested to contribute to serine phosphorylation of IRS proteins and is linked to insulin resistance (Bloch-Damti et al., 2006; Gupte et al., 2008), a decrease in Hsp25 expression could be also linked to IRS serine phosphorylation. We observed a decrease in the expression of Hsp25 in rats exhibiting both partial and full DA depletion. This could indicate increased vulnerability to oxidative stress, even in the absence of altered phosphorylation levels. Because the pool from which activated Hsp25 can be drawn is decreased, it is possible that the Hsp response upon exposure to stress conditions will be impaired, resulting in cellular and mitochondrial damage.

When given an IPGTT, severely depleted rats exhibited a nearly significant increase in serum insulin levels and a significant drop in blood glucose levels 15 minutes post-bolus compared to controls. Chronic hyperglycemia is often preceded by increased metabolic demand for insulin and compensation by beta cells to produce more insulin. This state of hyperinsulinemia typically precedes glucose intolerance (Smiley and Umpierrez, 2007). The changes we observe at 15 minutes post-bolus may indicate that changes in peripheral glucose tolerance are beginning to occur six weeks post-lesion. However, severely depleted rats are not glucose intolerant, as glucose and insulin levels are not different between groups at any other timepoint or over the course of the test. It is thus possible that changes in brain insulin signaling precede peripheral glucose intolerance.

Our statistical analyses revealed no effect of striatal hemisphere on any protein measures addressed here. Although we did not measure diffusion, it is highly unlikely that unilaterally administered 6-OHDA diffused into the contralateral hemisphere. Our findings therefore suggest that the between-groups differences in expression and activation of proteins involved in insulin signaling in this experiment are due to DA depletion rather than direct effects from the toxin. It has been shown that the contralateral striatum is affected by a unilateral 6-OHDA lesion even when DA projections to the contralateral striatum remain intact (Cadet et al., 1991; Lawler et al., 1995; Nikolaus et al., 2003). The effects of unilateral DA depletion are thus not necessarily restricted to the lesioned hemisphere, and the bilateral effects that we observe here warrant further investigation. Furthermore, 6-OHDA induced oxidative stress has been shown to return to pre-lesion levels within 7 days after administration (Sanchez-Iglesias et al., 2007). It is therefore also unlikely that a sufficient level of residual oxidative stress persists from 6-OHDA administration to affect these measures 6 weeks post-lesion.

Overall, our results demonstrate a bilateral increase in measures of striatal insulin resistance in rats exhibiting severe DA depletion, with some effects in animals with partial depletion. These novel findings suggest a direct effect of nigrostriatal DA depletion on insulin signaling in the basal ganglia. Although we cannot completely rule out a general neurotoxic effect of 6-OHDA on insulin signaling, several factors argue against this alternative hypothesis. The first two are that 6-OHDA is highly selective for catecholamines such as DA (Schober, 2004), and that DA terminals comprise less than 5% of striatal tissue content (Bennett and Wilson, 2000), where the measures of insulin resistance were made. Furthermore, measures of insulin resistance exhibited a "dose-dependent" effect, with the severely DA-depleted group exhibiting greater effects than the partially depleted group. These findings nevertheless warrant investigation of insulin signaling in other brain areas and in other preclinical models of PD.

Because the hypothalamus provides a direct connection to peripheral metabolism, future studies of whether this region is affected in the 6-OHDA model are also warranted. The extent of brain insulin resistance beyond basal ganglia nuclei could shed more light on the question of how PD can be a risk factor for peripheral glucose intolerance.

4. Materials and methods

4.1 Animals

Twenty male 4 month old Fisher 344 rats were obtained from National Institutes on Aging colonies (Harlan). Rats were housed two per cage, maintained on a 12 hour light/dark cycle, and provided food and water ad libitum. Protocols for animal use were approved by the University of Kansas Medical Center Institutional Animal Care and Use Committee and adhered to the Guide for the Care and Use of Laboratory Animals (National Research Council, 1996).

4.2 Materials

Antibodies against phospho-SAPK/JNK(T183/Y185), total SAPK/JNK, phospho-AKT, total AKT, and phospho-GSKα/β (Ser21/9) were obtained from Cell Signaling (Beverly, MA). Anti-phospho-Hsp 25 and anti-Hsp 25 were purchased from Stressgen (Victoria, BC, Canada). Anti-phospho-Ser307-IRS-1 and total GSK3-α/β were obtained from Upstate (Lake Placid, NY), while total IRS-1 was purchased from BD Biosciences (Franklin Lakes, NJ). Antibodies against phospho-Ser731-IRS-2 (corresponding to rat phospho-Ser233) and Actin were obtained from Abcam (Cambridge, MA). Goat-anti-rabbit HRP-conjugated secondary antibodies were purchased from Santa Cruz Biotechnology (Santa Cruz, CA). Goat anti-mouse HRP-conjugated secondary antibodies were obtained from Bio-Rad (Hercules, CA). Chemicals used in HPLC-EC (DA, DOPAC, DHBA) were obtained from Sigma-Aldrich (St. Louis, MO). Enhanced chemiluminescence reagents were purchased from Amersham (Little Chalfont, Buckinghamshire, UK).

4.3. 6-OHDA Infusion

The 6-OHDA lesion procedure was based on previously published studies (e.g. Enna et al., 2006). Rats were anesthetized with Nembutal (50mg/mL) at 1mL/kg body weight prior to surgery and placed into a stereotaxic frame. Rats in the lesion group (n=14) were infused with 4uL of 6-OHDA in 0.9% NaCl with 0.02% ascorbate into the right medial forebrain bundle (stereotaxic coordinates with respect to bregma: M/L 1.3, A/P −4.4, and D/V −7.8) at a dose of 2.25mg/mL. The infusion rate was 0.25uL/minute over a period of 16 minutes, a flow rate that will limit local tissue damage. The cannula was withdrawn 1 minute after infusion was completed. Identical surgical procedure was followed for rats receiving a sham lesion (n=6), except that sham rats received saline (0.9% NaCl with 0.02% ascorbate) instead of 6-OHDA. Rats were allowed to recover for six weeks post-surgery. The six-week timepoint is a somewhat arbitrary timepoint that was chosen to ensure that the oxidative stress and apoptotic and neurodegenerative processes in the nigrostriatal pathway following 6-OHDA administration were completed.

4.4. Intraperitoneal glucose tolerance test (IPGTT)

An IPGTT was performed 48 hours before animals were sacrificed. Animals were fasted overnight (12 hours) prior to the IPGTT. A 60% glucose bolus of D-(+)-Glucose (Sigma) in saline was administered intraperitoneally at t=0. A glucometer (AccuCheck Active) was used to analyze glucose levels in tail blood at timepoints 0,15, 30, 60, 90, and 120 minutes following glucose administration. Tail blood samples (~400μL) were taken at each timepoint and allowed to clot on ice for 30 minutes before being centrifuged at 3,000 × g for 1 hour. Serum was

immediately extracted and aliquoted into fresh tubes. Serum insulin was measured using an Insulin (rat) EIA kit (Alpco Diagnostics). Rats were anesthetized with Nembutal (50mg/mL) at 1mL/Kg body weight 45 minutes prior to the IPGTT.

4.5. HPLC-EC analysis of Dopamine Content

The HPLC-EC system consisted of a Coulochem III electrochemical detector (ESA), Model 5011A high-sensitivity analytical coulometric cell (ESA), LC-10AS single plunger pump (Shimadzu), and 3μm CAPCELL PAK reversed phase C-18 column (Shiseido). The composition of citrate acetate mobile phase (pH 4) was as follows: octane sulfonic acid (0.0738 g/L), ethylenediaminetetraacetic acid (0.05 g/L), sodium acetate trihydrate (13.8 g/L), citric acid (14 g/L), triethylamine (0.01%), and methanol (4%). Mobile phase was made using filtered water from a Milli-Q purification system (Millipore) and the solution was subsequently filtered through a 0.2μm nylon membrane filter (Whatman).

Six weeks post-lesion, rats were sacrificed and brains were removed. Bilateral striatum samples were dissected, weighed, and frozen on dry ice to be processed for HPLC-EC and Western blot analysis. Striatal sections were processed for HPLC through sonication in burnt, filtered citrate acetate mobile phase with 50uL DHBA (0.1mM) added to each sample. Following sonication, tubes were centrifuged in a Hermle Z400K refrigerated centrifuge (Midwest Scientific) for 10 minutes at 12,000 × g at 4°C. Supernatants were extracted and placed into Microcon Ultracel YM-10 centrifugal filter devices (Amicon), and centrifuged at 12,000 × g for 1 hour at 4°C. Eluent was collected and used for HPLC analyses. DA depletion values were obtained from HPLC measures by dividing the DA content of the striatum on the lesioned (right) side by the DA content of the striatum on the non-lesioned (left) side of the brain. Rats receiving a lesion were further divided into two groups (partial and severe DA depletion) based upon DA depletion levels.

4.6. Western Immunoblotting

Protein samples were processed as previously described (Geiger et al., 2007; Gupte et al., 2008). Frozen striatum samples to be processed for protein analysis were diluted 10× in cell extraction buffer (Invitrogen) with protease inhibitor cocktail (500μL, Invitrogen), sodium flouride (200mM), sodium orthovanodate (200mM) and phenylmethanesulphonylfluoride (200mM) added. Tissue was homogenized using a hand homogenizer, and samples were placed on ice for 1 hour with intermittent vortexing to allow protein extraction to occur. Samples were centrifuged at 3,000 ×g at 4°C for 20 minutes. Supernatants were extracted and placed into fresh tubes.

A Bradford assay was performed to determine sample protein concentrations. Samples were analyzed in triplicate using working strength Bradford reagent, diluted 5x from Bradford dye concentrate (BioRad) with filtered distilled water. Based upon protein concentrations, samples were diluted with HES buffer (20mM HEPES, 1mM EDTA, 250M Sucrose, pH 7.4) and reducing sample buffer (0.3M Tris-HCL, 5% SDS, 50% glycerol, 100mM dithiothreitol, Thermo Scientific) to obtain samples of constant concentration for analysis using SDS-PAGE. Due to the large molecular weight of the IRS proteins, samples analyzed for IRS1 and IRS2 phosphorylation and expression were run on 7.5% gels. When examining all other proteins of interest, samples were run on 10% gels.

For SDS-PAGE, the largest number of samples were run on the same gel as possible. After SDS-PAGE, samples were transferred to nitrocellulose membranes. Due to the high molecular weight of IRS2, gels to analyze IRS2 total protein and serine phosphorylation were transferred for 90 minutes at 400mA. All other proteins were transferred for 60 minutes at 200mA. Nitrocellulose membranes were blocked in 5% nonfat dry milk for 1 hour and incubated with

primary antibody diluted 1:1000 in 1% milk overnight at 4°C. Secondary antibody corresponding to the host primary antibody of interest was used at a dilution of 1:10,000 in 1% milk for 1 hour at room temperature. Upon exposure, films were scanned at high resolution to obtain digital images. Densitometry analyses were performed using Image J software. Images were normalized for background and repeated densitometry measurements were averaged for each band of interest. All bands of interest shown in figures are taken from the same gel. For analysis of results, phosphorylated protein levels were normalized to total protein levels, while total protein expression was normalized to the loading control actin.

4.7. Statistical analysis

Two-way analysis of variance (ANOVA) with striatal hemisphere and experimental group as factors was used to analyze differences in protein expression and activation between sham, partial, and severe lesion groups. No protein expression or activation differences between lesioned and non-lesioned hemispheres were observed for any measure analyzed, so measurements from the left and right striatal hemisphere were averaged to obtain one data point for each animal. ANOVA was used to analyze IRS2 serine phosphorylation and expression, and when appropriate this was followed by a post hoc comparison using the least-significant difference test. Low tissue weights of several animals from the partial depletion group resulted in a lower partial lesion group n-value (N=3) for other proteins analyzed. To account for this, we used nonparametric statistics (Kruskal-Wallis One-Way Analysis of Variance) to analyze measures other than phosphorylated and total IRS2. Multivariate repeated measures analysis was used to compare insulin and glucose levels over the course of an IPGTT, and an unpaired Student's t-test was used to analyze differences between groups at individual time points during the IPGTT. For all analyses, statistical significance was set at $P \leq 0.05$.

Acknowledgments

The authors would like to acknowledge Susan Smittkamp and Brittany Gorres for their technical assistance with this manuscript. This study was supported by NIH grants AG023549, AG026491, a Kansas City Area Life Sciences Institute Development Grant, and the Smith Intellectual and Developmental Disabilities Research Center (HD02528).

References

Aguirre V, Werner ED, Giraud J, Lee YH, Shoelson SE, White MF. Phosphorylation of Ser307 in insulin receptor substrate-1 blocks interactions with the insulin receptor and inhibits insulin action. J Biol Chem 2002;277:1531–1537. [PubMed: 11606564]

Barbeau A, Pourcher E. New data on the genetics of Parkinson's disease. Can J Neurol Sci 1982;9:53–60. [PubMed: 7093827]

Baum L, Hansen L, Masliah E, Saitoh T. Glycogen synthase kinase 3 alteration in Alzheimer disease is related to neurofibrillary tangle formation. Mol Chem Neuropathol 1996;29:253–261. [PubMed: 8971700]

Beal MF. Mitochondria, oxidative damage, and inflammation in Parkinson's disease. Ann N Y Acad Sci 2003;991:120–131. [PubMed: 12846981]

Bennett, BD.; Wilson, CJ. Synaptology and physiology of neostriatal neurones. In: Miller, R.; Wickens, JR., editors. Brain Dynamics and the Striatal Complex. Australia: Harwood Academic Publishers; 2000. p. 11-140.

Bloch-Damti A, Bashan N. Proposed mechanisms for the induction of insulin resistance by oxidative stress. Antioxid Redox Signal 2005;7:1553–1567. [PubMed: 16356119]

Bloch-Damti A, Potashnik R, Gual P, Le Marchand-Brustel Y, Tanti JF, Rudich A, Bashan N. Differential effects of IRS1 phosphorylated on Ser307 or Ser632 in the induction of insulin resistance by oxidative stress. Diabetologia 2006;49:2463–2473. [PubMed: 16896943]

Boyd AE 3rd, Lebovitz HE, Feldman JM. Endocrine function and glucose metabolism in patients with Parkinson's disease and their alternation by L-Dopa. J Clin Endocrinol Metab 1971;33:829–837. [PubMed: 5125386]

Cadet JL, Kujirai K, Przedborski S. Bilateral modulation of [3H]neurotensin binding by unilateral intrastriatal 6-hydroxydopamine injections: evidence from a receptor autoradiographic study. Brain Res 1991;564:37–44. [PubMed: 1663814]

Chen G, Bower KA, Ma C, Fang S, Thiele CJ, Luo J. Glycogen synthase kinase 3beta (GSK3beta) mediates 6-hydroxydopamine-induced neuronal death. Faseb J 2004;18:1162–1164. [PubMed: 15132987]

Dong X, Park S, Lin X, Copps K, Yi X, White MF. Irs1 and Irs2 signaling is essential for hepatic glucose homeostasis and systemic growth. J Clin Invest 2006;116:101–114. [PubMed: 16374520]

Downs CA, Jones LR, Heckathorn SA. Evidence for a novel set of small heat-shock proteins that associates with the mitochondria of murine PC12 cells and protects NADH:ubiquinone oxidoreductase from heat and oxidative stress. Arch Biochem Biophys 1999;365:344–350. [PubMed: 10328830]

El Messari S, Leloup C, Quignon M, Brisorgueil MJ, Penicaud L, Arluison M. Immunocytochemical localization of the insulin-responsive glucose transporter 4 (Glut4) in the rat central nervous system. J Comp Neurol 1998;399:492–512. [PubMed: 9741479]

Enna SJ, Reisman SA, Stanford JA. CGP 56999A, a GABA(B) receptor antagonist, enhances expression of brain-derived neurotrophic factor and attenuates dopamine depletion in the rat corpus striatum following a 6-hydroxydopamine lesion of the nigrostriatal pathway. Neurosci Lett 2006;406:102–106. [PubMed: 16890350]

Escobedo J, Pucci AM, Koh TJ. HSP25 protects skeletal muscle cells against oxidative stress. Free Radic Biol Med 2004;37:1455–1462. [PubMed: 15454285]

Figlewicz DP, Evans SB, Murphy J, Hoen M, Baskin DG. Expression of receptors for insulin and leptin in the ventral tegmental area/substantia nigra (VTA/SN) of the rat. Brain Res 2003;964:107–115. [PubMed: 12573518]

Fink RI, Kolterman OG, Griffin J, Olefsky JM. Mechanisms of insulin resistance in aging. J Clin Invest 1983;71:1523–1535. [PubMed: 6345584]

Garcia-Segura LM, Diz-Chaves Y, Perez-Martin M, Darnaudery M. Estradiol, insulin-like growth factor-I and brain aging. Psychoneuroendocrinology 2007;32:S57–S61. [PubMed: 17618061]

Garcia BG, Wei Y, Moron JA, Lin RZ, Javitch JA, Galli A. Akt is essential for insulin modulation of amphetamine-induced human dopamine transporter cell-surface redistribution. Mol Pharmacol 2005;68:102–109. [PubMed: 15795321]

Geiger PC, Hancock C, Wright DC, Han DH, Holloszy JO. IL-6 increases muscle insulin sensitivity only at superphysiological levels. Am J Physiol Endocrinol Metab 2007;292:E1842–E1846. [PubMed: 17327367]

Gupte AA, Bomhoff GL, Geiger PC. Age-related differences in skeletal muscle insulin signaling: the role of stress kinases and heat shock proteins. J Appl Physiol. 2008

Henriksen EJ, Kinnick TR, Teachey MK, O'Keefe MP, Ring D, Johnson KW, Harrison SD. Modulation of muscle insulin resistance by selective inhibition of GSK-3 in Zucker diabetic fatty rats. Am J Physiol Endocrinol Metab 2003;284:E892–E900. [PubMed: 12517738]

Hudson JL, van Horne CG, Stromberg I, Brock S, Clayton J, Masserano J, Hoffer BJ, Gerhardt GA. Correlation of apomorphine- and amphetamine-induced turning with nigrostriatal dopamine content in unilateral 6-hydroxydopamine lesioned rats. Brain Res 1993;626:167–174. [PubMed: 8281427]

Kim B, van Golen CM, Feldman EL. Insulin-like growth factor I induces preferential degradation of insulin receptor substrate-2 through the phosphatidylinositol 3-kinase pathway in human neuroblastoma cells. Endocrinology 2005;146:5350–5357. [PubMed: 16150916]

Klintworth H, Newhouse K, Li T, Choi WS, Faigle R, Xia Z. Activation of c-Jun N-terminal protein kinase is a common mechanism underlying paraquat- and rotenone-induced dopaminergic cell apoptosis. Toxicol Sci 2007;97:149–162. [PubMed: 17324951]

Lawler CP, Gilmore JH, Watts VJ, Walker QD, Southerland SB, Cook LL, Mathis CA, Mailman RB. Interhemispheric modulation of dopamine receptor interactions in unilateral 6-OHDA rodent model. Synapse 1995;21:299–311. [PubMed: 8869160]

Lee J, Kim MS. The role of GSK3 in glucose homeostasis and the development of insulin resistance. Diabetes Res Clin Pract 2007;77:S49–S57. [PubMed: 17478001]

Leroy K, Brion JP. Developmental expression and localization of glycogen synthase kinase-3beta in rat brain. J Chem Neuroanat 1999;16:279–293. [PubMed: 10450875]

Liberman Z, Plotkin B, Tennenbaum T, Eldar-Finkelman H. Coordinated phosphorylation of insulin receptor substrate-1 by glycogen synthase kinase-3 and protein kinase C betaII in the diabetic fat tissue. Am J Physiol Endocrinol Metab 2008;294:E1169–E1177. [PubMed: 18430969]

Lin X, Taguchi A, Park S, Kushner JA, Li F, Li Y, White MF. Dysregulation of insulin receptor substrate 2 in beta cells and brain causes obesity and diabetes. J Clin Invest 2004;114:908–916. [PubMed: 15467829]

Lipman IJ, Boykin ME, Flora RE. Glucose intolerance in Parkinson's disease. J Chronic Dis 1974;27:573–579. [PubMed: 4436423]

Moroo I, Yamada T, Makino H, Tooyama I, McGeer PL, McGeer EG, Hirayama K. Loss of insulin receptor immunoreactivity from the substantia nigra pars compacta neurons in Parkinson's disease. Acta Neuropathol 1994;87:343–348. [PubMed: 8017169]

Morton JP, Maclaren DP, Cable NT, Campbell IT, Evans L, Bongers T, Griffiths RD, Kayani AC, McArdle A, Drust B. Elevated core and muscle temperature to levels comparable to exercise do not increase heat shock protein content of skeletal muscle of physically active men. Acta Physiol (Oxf) 2007;190:319–327. [PubMed: 17488245]

Nikolaus S, Larisch R, Beu M, Forutan F, Vosberg H, Muller-Gartner HW. Bilateral increase in striatal dopamine D2 receptor density in the 6-hydroxydopamine-lesioned rat: a serial in vivo investigation with small animal PET. Eur J Nucl Med Mol Imaging 2003;30:390–395. [PubMed: 12634967]

Papapetropoulos S, Ellul J, Argyriou AA, Talelli P, Chroni E, Papapetropoulos T. The effect of vascular disease on late onset Parkinson's disease. Eur J Neurol 2004;11:231–235. [PubMed: 15061824]

Pardini AW, Nguyen HT, Figlewicz DP, Baskin DG, Williams DL, Kim F, Schwartz MW. Distribution of insulin receptor substrate-2 in brain areas involved in energy homeostasis. Brain Res 2006;1112:169–178. [PubMed: 16925984]

Park KJ, Gaynor RB, Kwak YT. Heat shock protein 27 association with the I kappa B kinase complex regulates tumor necrosis factor alpha-induced NF-kappa B activation. J Biol Chem 2003;278:35272–35278. [PubMed: 12829720]

Paz K, Hemi R, LeRoith D, Karasik A, Elhanany E, Kanety H, Zick Y. A molecular basis for insulin resistance. Elevated serine/threonine phosphorylation of IRS-1 and IRS-2 inhibits their binding to the juxtamembrane region of the insulin receptor and impairs their ability to undergo insulin-induced tyrosine phosphorylation. J Biol Chem 1997;272:29911–29918. [PubMed: 9368067]

Pederson TM, Kramer DL, Rondinone CM. Serine/threonine phosphorylation of IRS-1 triggers its degradation: possible regulation by tyrosine phosphorylation. Diabetes 2001;50:24–31. [PubMed: 11147790]

Peng J, Andersen JK. The role of c-Jun N-terminal kinase (JNK) in Parkinson's disease. IUBMB Life 2003;55:267–271. [PubMed: 12880208]

Porte D Jr, Baskin DG, Schwartz MW. Insulin signaling in the central nervous system: a critical role in metabolic homeostasis and disease from C. elegans to humans. Diabetes 2005;54:1264–1276. [PubMed: 15855309]

Pressley JC, Louis ED, Tang MX, Cote L, Cohen PD, Glied S, Mayeux R. The impact of comorbid disease and injuries on resource use and expenditures in parkinsonism. Neurology 2003;60:87–93. [PubMed: 12525724]

Rawal N, Parish C, Castelo-Branco G, Arenas E. Inhibition of JNK increases survival of transplanted dopamine neurons in Parkinsonian rats. Cell Death Differ 2007;14:381–383. [PubMed: 16858428]

Reagan LP. Neuronal insulin signal transduction mechanisms in diabetes phenotypes. Neurobiol Aging 2005;26:56–59. [PubMed: 16225964]

Rui L, Fisher TL, Thomas J, White MF. Regulation of insulin/insulin-like growth factor-1 signaling by proteasome-mediated degradation of insulin receptor substrate-2. J Biol Chem 2001;276:40362–40367. [PubMed: 11546773]

Rui L, Yuan M, Frantz D, Shoelson S, White MF. SOCS-1 and SOCS-3 block insulin signaling by ubiquitin-mediated degradation of IRS1 and IRS2. J Biol Chem 2002;277:42394–42398. [PubMed: 12228220]

Sanchez-Iglesias S, Rey P, Mendez-Alvarez E, Labandeira-Garcia JL, Soto-Otero R. Time-course of brain oxidative damage caused by intrastriatal administration of 6-hydroxydopamine in a rat model of Parkinson's disease. Neurochem Res 2007;32:99–105. [PubMed: 17160721]

Sandyk R. The relationship between diabetes mellitus and Parkinson's disease. Int J Neurosci 1993;69:125–130. [PubMed: 8082998]

Sawka-Verhelle D, Baron V, Mothe I, Filloux C, White MF, Van Obberghen E. Tyr624 and Tyr628 in insulin receptor substrate-2 mediate its association with the insulin receptor. J Biol Chem 1997;272:16414–16420. [PubMed: 9195949]

Schober A. Classic toxin-induced animal models of Parkinson's disease: 6-OHDA and MPTP. Cell Tissue Res 2004;318:215–224. [PubMed: 15503155]

Sharfi H, Eldar-Finkelman H. Sequential phosphorylation of insulin receptor substrate-2 by glycogen synthase kinase-3 and c-Jun NH2-terminal kinase plays a role in hepatic insulin signaling. Am J Physiol Endocrinol Metab 2008;294:E307–E315. [PubMed: 18029441]

Sirtori CR, Bolme P, Azarnoff DL. Metabolic responses to acute and chronic L-dopa administration in patients with parkinsonism. N Engl J Med 1972;287:729–733. [PubMed: 5056733]

Skitek EB, Fowler SC, Tessel RE. Effects of unilateral striatal dopamine depletion on tongue force and rhythm during licking in rats. Behav Neurosci 1999;113:567–573. [PubMed: 10443783]

Smiley D, Umpierrez G. Metformin/rosiglitazone combination pill (Avandamet) for the treatment of patients with Type 2 diabetes. Expert Opin Pharmacother 2007;8:1353–1364. [PubMed: 17563269]

Smith JL, Ju JS, Saha BM, Racette BA, Fisher JS. Levodopa with carbidopa diminishes glycogen concentration, glycogen synthase activity, and insulin-stimulated glucose transport in rat skeletal muscle. J Appl Physiol 2004;97:2339–2346. [PubMed: 15258132]

Sykiotis GP, Papavassiliou AG. Serine phosphorylation of insulin receptor substrate-1: a novel target for the reversal of insulin resistance. Mol Endocrinol 2001;15:1864–1869. [PubMed: 11682617]

Taguchi A, Wartschow LM, White MF. Brain IRS2 signaling coordinates life span and nutrient homeostasis. Science 2007;317:369–372. [PubMed: 17641201]

Takahashi M, Yamada T, Tooyama I, Moroo I, Kimura H, Yamamoto T, Okada H. Insulin receptor mRNA in the substantia nigra in Parkinson's disease. Neurosci Lett 1996;204:201–204. [PubMed: 8938265]

Uyama N, Geerts A, Reynaert H. Neural connections between the hypothalamus and the liver. Anat Rec A Discov Mol Cell Evol Biol 2004;280:808–820. [PubMed: 15382020]

van der Heide LP, Ramakers GM, Smidt MP. Insulin signaling in the central nervous system: learning to survive. Prog Neurobiol 2006;79:205–221. [PubMed: 16916571]

Wang Q, Somwar R, Bilan PJ, Liu Z, Jin J, Woodgett JR, Klip A. Protein kinase B/Akt participates in GLUT4 translocation by insulin in L6 myoblasts. Mol Cell Biol 1999;19:4008–4018. [PubMed: 10330141]

Werner ED, Lee J, Hansen L, Yuan M, Shoelson SE. Insulin resistance due to phosphorylation of insulin receptor substrate-1 at serine 302. J Biol Chem 2004;279:35298–35305. [PubMed: 15199052]

White MF. The IRS-signalling system: a network of docking proteins that mediate insulin action. Mol Cell Biochem 1998;182:3–11. [PubMed: 9609109]

Wilhelm KR, Yanamandra K, Gruden MA, Zamotin V, Malisauskas M, Casaite V, Darinskas A, Forsgren L, Morozova-Roche LA. Immune reactivity towards insulin, its amyloid and protein S100B in blood sera of Parkinson's disease patients. Eur J Neurol 2007;14:327–334. [PubMed: 17355556]

Yuan H, Sarre S, Ebinger G, Michotte Y. Histological, behavioural and neurochemical evaluation of medial forebrain bundle and striatal 6-OHDA lesions as rat models of Parkinson's disease. J Neurosci Methods 2005;144:35–45. [PubMed: 15848237]

Zhande R, Mitchell JJ, Wu J, Sun XJ. Molecular mechanism of insulin-induced degradation of insulin receptor substrate 1. Mol Cell Biol 2002;22:1016–1026. [PubMed: 11809794]

Zick Y. Ser/Thr phosphorylation of IRS proteins: a molecular basis for insulin resistance. Sci STKE 2005;2005:pe4. [PubMed: 15671481]

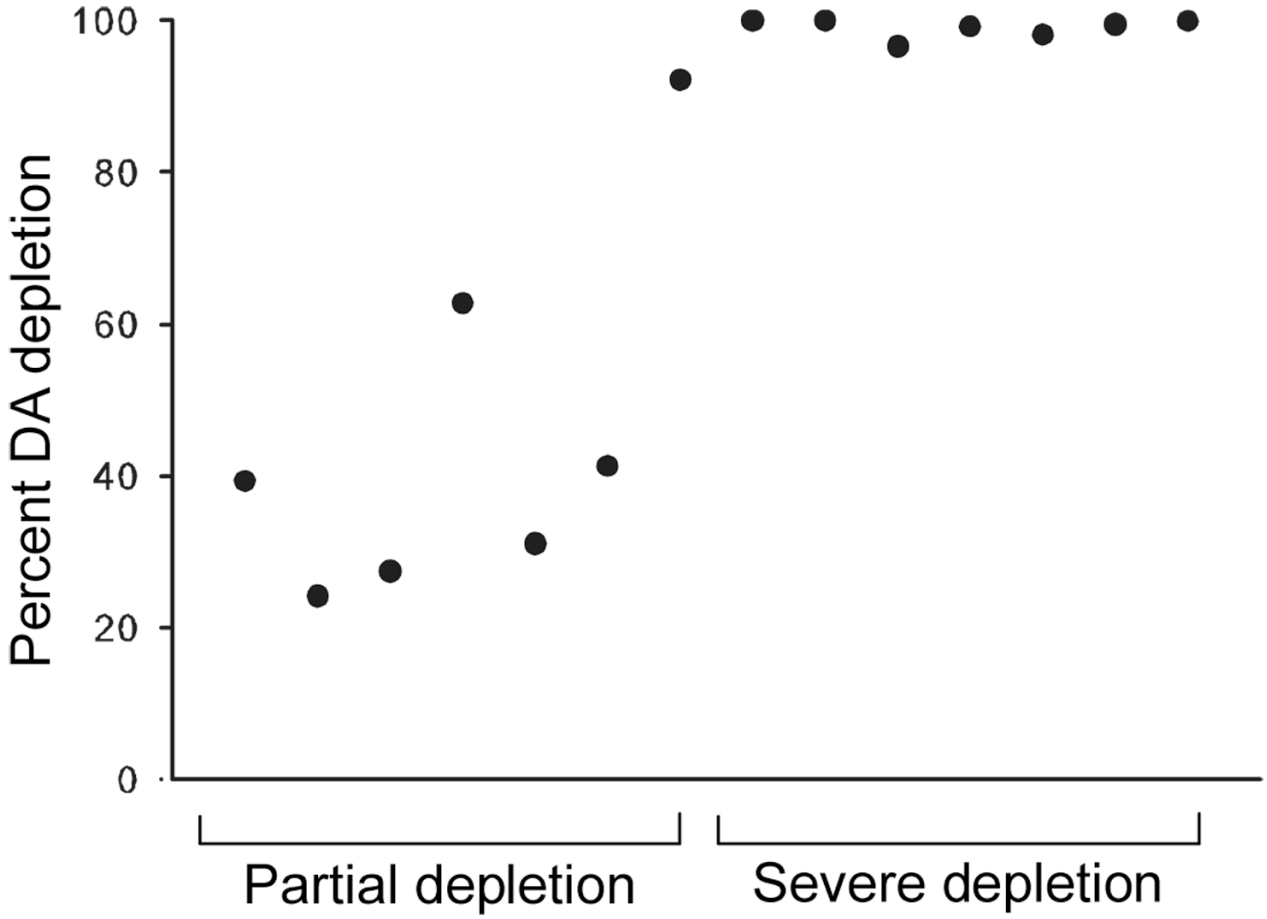

Figure 1. DA depletion levels for partially and severely depleted rats

DA content in the right (lesioned) striatum was divided by DA levels in left (nonlesioned) striatum to obtain a percent depletion for each lesioned rat. The average depletion level for rats with partial DA depletion was 37.6% ± 13.9, while rats in the severe DA depletion group exhibited a mean depletion of 98% ± 2.7%.

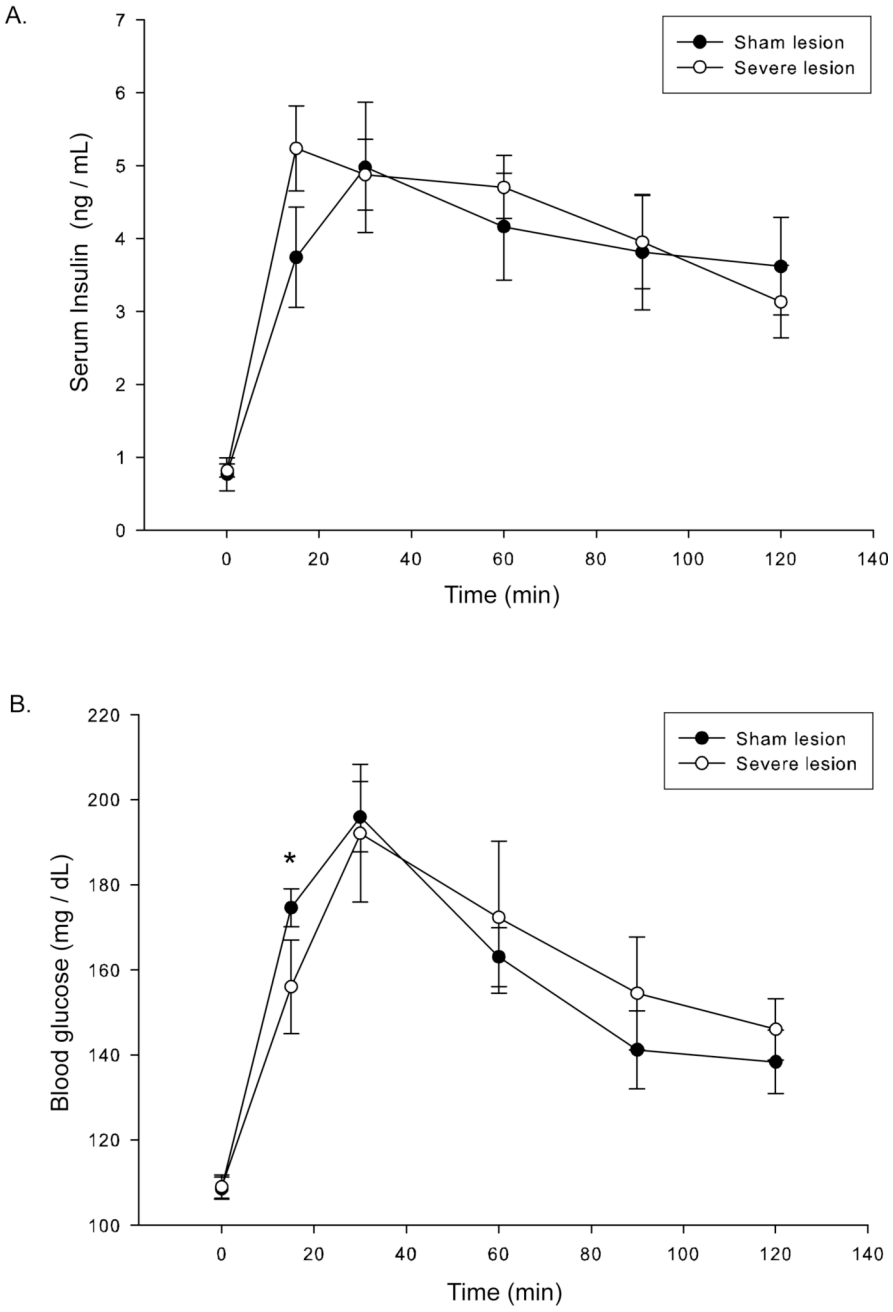

Figure 2. Intraperitoneal glucose tolerance test (IPGTT)

After an overnight (12 hour) fast, an intraperitoneal injection of 60% glucose was administered at 2g glucose/kg body weight. Insulin **(A)** and glucose **(B)** were measured in tail blood at six time points: 0,15,45,60, 90, and 120 minutes after the glucose bolus (injection at t=0). Fifteen minutes following the bolus, an increase in insulin that approaches significance (p=0.06) is reflected by a significant decrease in glucose (p=0.04). However, neither insulin nor glucose levels were significantly different between groups over the course of the test or at any other timepoint, indicating that severely depleted rats were not glucose intolerant six weeks postlesion. *P≤0.05.

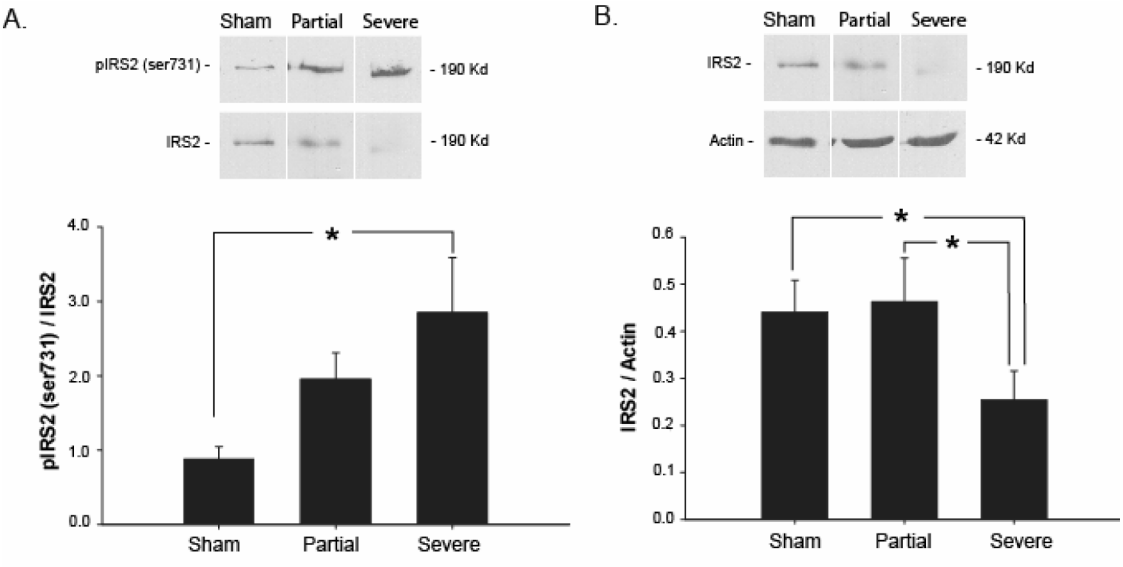

Figure 3. Effect of 6-OHDA lesion on IRS2 activation and protein content

Homogenized striatal lysates were analyzed by Western blot for pIRS2 **(A)**, normalized to total IRS2, and total IRS2 **(B)**, normalized to actin. There was a DA depletion-related increase in pIRS2, while total IRS2 was diminished in the severe lesion group. Values are means ± SE for 6–8 samples per group. *P≤0.05.

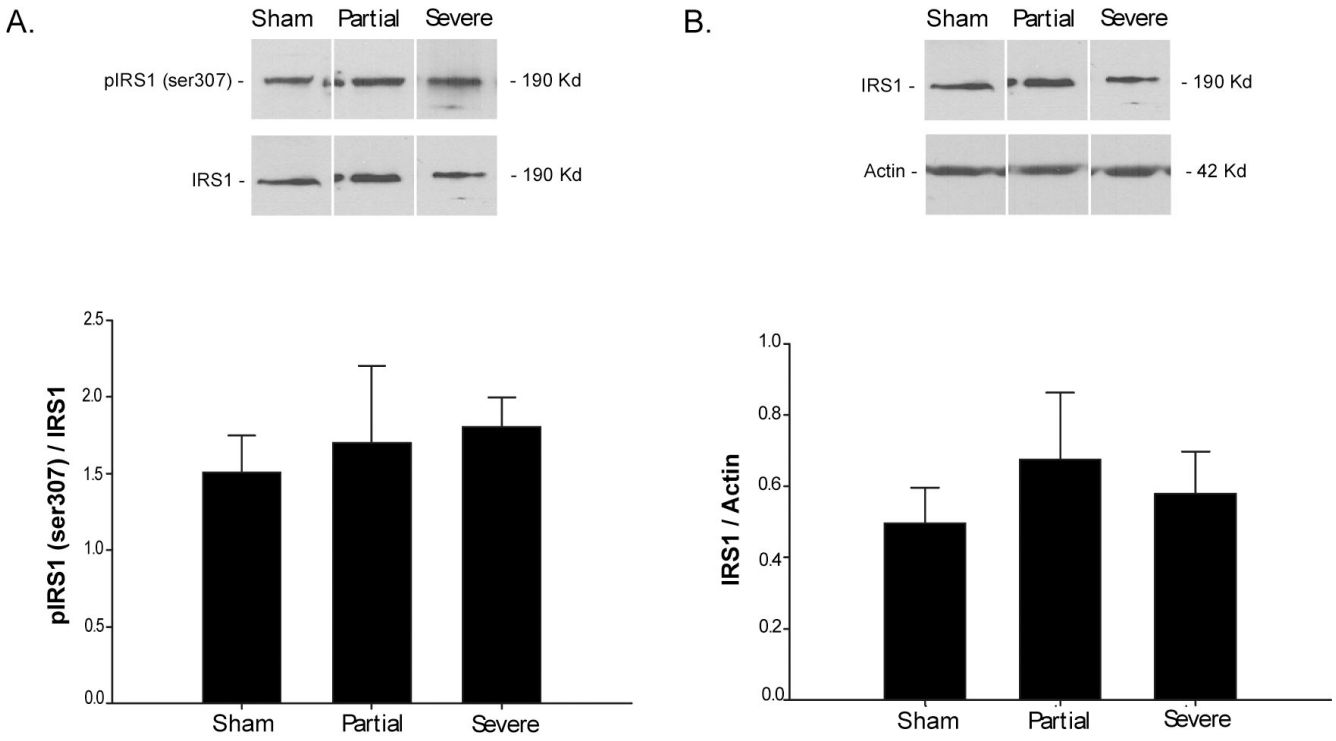

Figure 4. Protein expression and phosphorylation of IRS1

Homogenized striatal lysates were analyzed by Western blot for pIRS1 **(A)**, normalized to total IRS1, and total IRS1 **(B)**, normalized to actin. There was no significant difference between phosphorylated IRS1 or total IRS1 protein between any groups tested. Values are means ± SE for 3–8 samples per group.

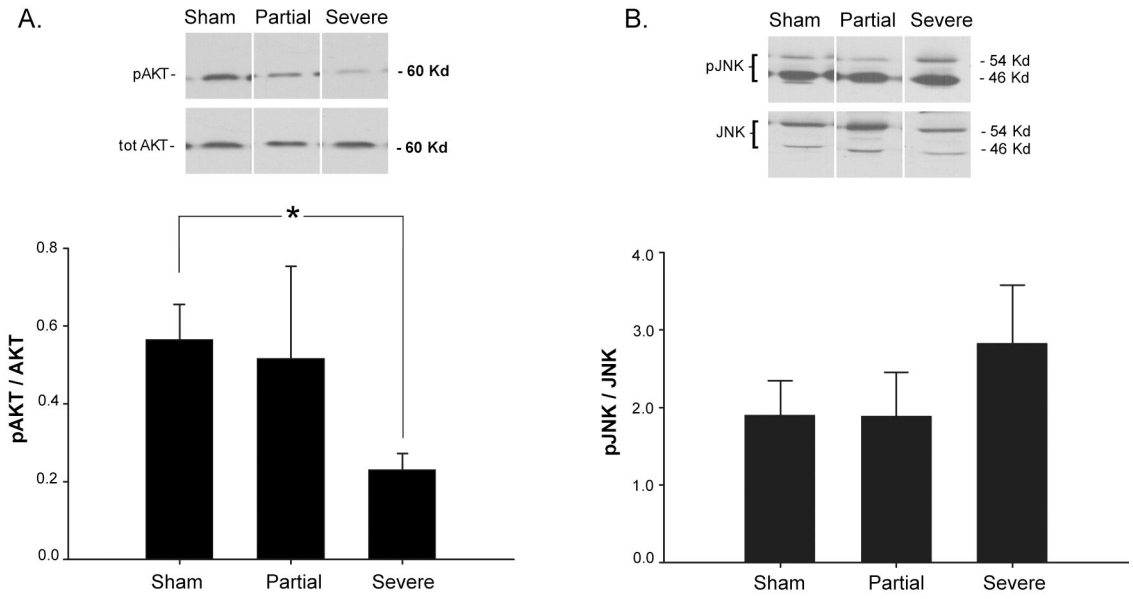

Figure 5. Activation of AKT and JNK

Homogenized striatal lysates were analyzed by Western blot for pAKT **(A)**, normalized to total AKT, and pJNK **(B)**, normalized to total JNK. pAKT was significantly decreased with a severe lesion when compared to sham lesion controls. Severely depleted rats also exhibited a non-significant increase in JNK phosphorylation. Values are means ± SE for 3–8 samples per group. *P≤0.05.

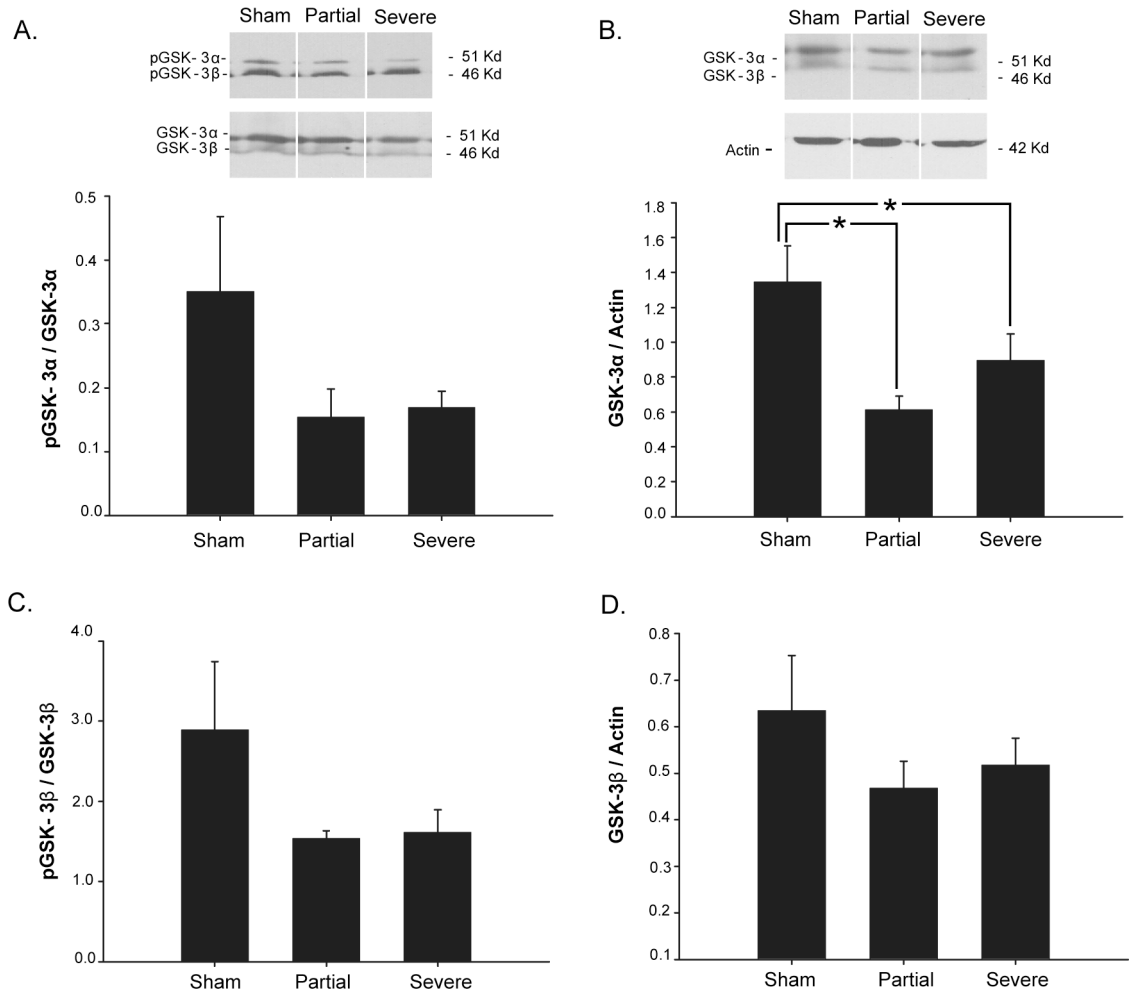

Figure 6. Activation of GSK3 isoforms in response to DA depletion

Homogenized striatal lysates were analyzed by Western blot for pGSK3-α **(A)**, normalized to total GSK3-α, GSK3-α **(B)**, normalized to actin, pGSK3-β **(C)**, normalized to total GSK3-β, and total GSK3-β **(D)**, normalized to actin. Total GSK3-α was decreased significantly in both the partial and severe lesion groups. Although pGSK3-α, pGSK3-β, and total GSK3-β were decreased in the lesioned groups, these effects did not reach significance. Values are means ± SE for 3–8 samples per group. *P≤0.05.

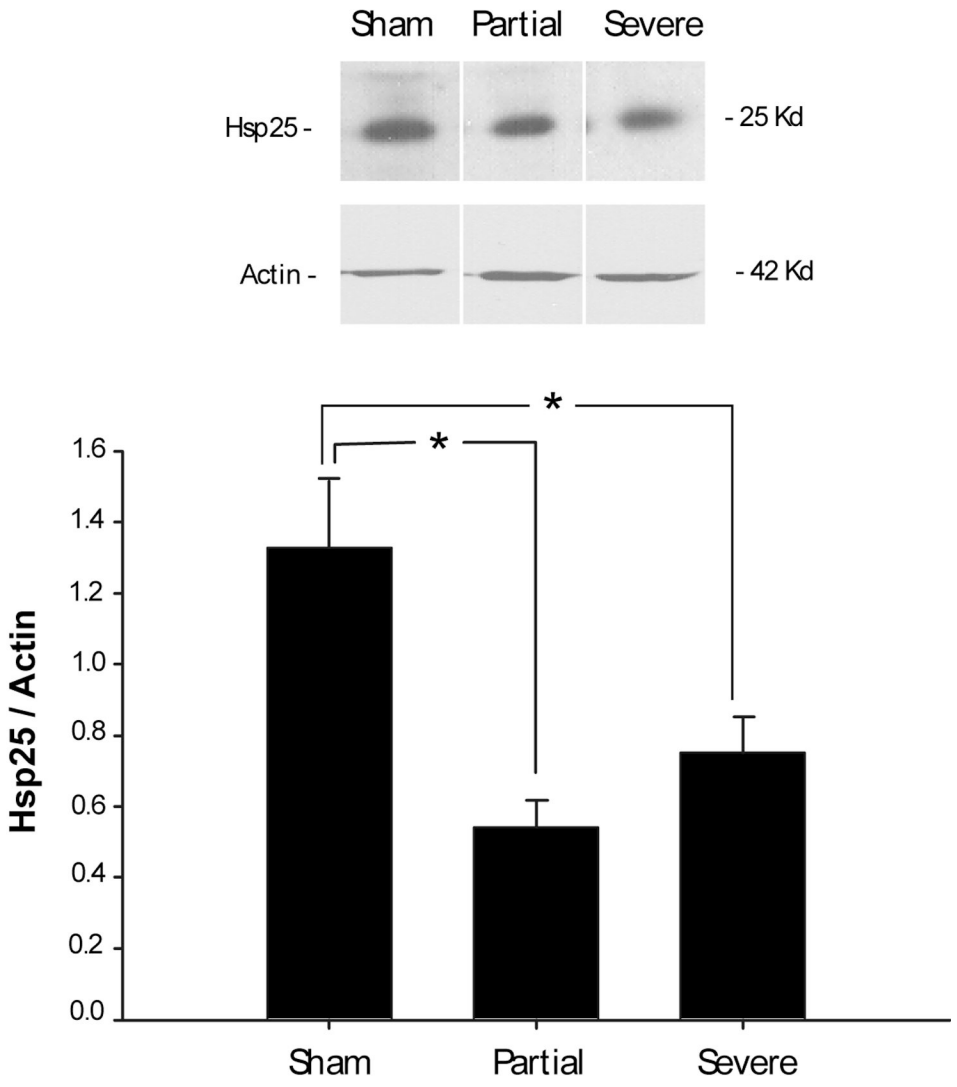

Figure 7. Expression of Hsp25 in response to a 6-OHDA lesion

Homogenized striatal lysates were analyzed for Hsp25 normalized to actin. Hsp25 was decreased significantly in both the partial and the severe lesion groups when compared to sham lesioned controls. Values are means ± SE for 3–8 samples per group. *P≤0.05.

Table 1

Mean (+/− S.E.M.) striatal DA and DOPAC values for experimental groups

	DOPAC (ng/g)		DA (ng/g)	
	Left Striatum	**Right Striatum**	**Left Striatum**	**Right Striatum**
Sham	1357.8 ± 130.3	1343.8 ± 117.4	4964.4 ± 383.4	4108.3 ± 584.3
Partial	1965.4 ± 419.4	2825.9 ± 597.2	4659.6 ±1057.0	2891.9 ± 693.8
Severe	1558.3 ± 169.9	85.3 ± 54.5	6852.8 ± 2450.9	210.4 ± 124.8